As mentioned earlier, the main advantage of this type of patch lies in its single-layer structure, which allows coplanar etching. The arrays thus obtained are structurally simple, of low thickness, and can be laid or conformed over a carrier structure of any shape: cylindrical, conical, spherical, etc.

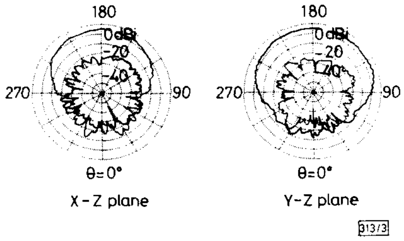

Fig. 3 *Radiation pattern of microstrip patch antenna*
a X–Z plane ($\phi = 0°$)
b Y–Z plane ($\phi = 90°$)
——— $E\theta$
------- $E\phi$

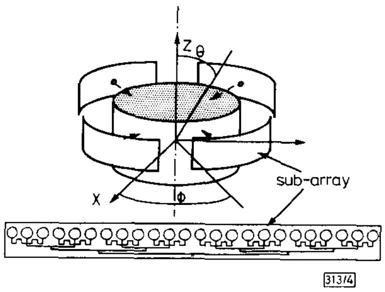

Fig. 4 *Microstrip belt antenna*

Application: The application developed at Aerospatiale Cannes, France, is a belt antenna conformed over a cylindrical structure to obtain as regular an omnidirectional pattern as possible. As the carrier structure has to face high dynamic loads, fast pressure variations and strong laminar flows, multilayer techniques cannot be used for this application.

The overall antenna is made up of four 24 element arrays as described above, uniformly fed, and spaced by half a wavelength as shown in Fig. 4. The pattern achieved thereby is given in Fig. 5. The antenna bandwidth for a voltage standing wave ratio (VSWR) lower than 2·0 can be as high as 7%.

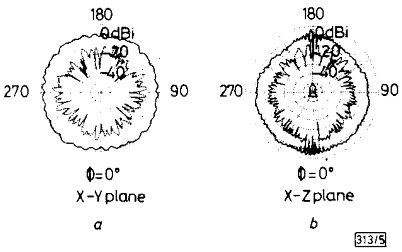

Fig. 5 *Radiation pattern of microstrip belt antenna*
a X–Y plane ($\theta = 90°$)
b X–Z plane ($\phi = 0°$)
——— $E\theta$
------- $E\phi$

Conclusion: The innovative radiating element presented here provides bandwidths that are several times those obtained with conventional patches. In addition, its simplicity of design, combining single-layer technology and a coplanar feeding concept, is ideally suited to applications in which severe aerodynamic constraints are involved.

One application is presented of a microstrip belt antenna that uses the radiating element concept described here, leading to outstanding bandwidth and radiation pattern performances.

8th June 1993

R. Buralli and M. Sauvan (*Aerospatiale, Espace et Défense, BP 99, 06322 Cannes-La-Bocca Cedex, France*)

Reference

1 HENDERSON, A., JAMES, J. R., and HALL, C. M.: 'Bandwidth extension techniques in printed conformal antennas', *Military Microwaves*, 1986, pp. 329–334

STRICT CALCULATION OF THE LIGHT STATISTICS AT THE OUTPUT OF A TRAVELLING WAVE OPTICAL AMPLIFIER

J. Guitart and S. Ruiz-Moreno

Indexing terms: Laser theory, Optical amplifiers, Travelling-wave semiconductor amplifiers

A new method for calculating the probability density function of the photon number propagating through a travelling wave optical amplifier with no restriction on its working regime (linear and nonlinear) is reported. The Letter shows that the widely used Gaussian approximation of the probability density function does not match the real statistics if the incident optical power is small.

Introduction: The statistical behaviour of a travelling wave optical amplifier (TWOA) can be described through the photon density matrix equation (PDME) [1–4]. Its diagonal elements give the differential equation for the probability density function, $P_{n,m}(z)$, as having m photons in the considered mode in the propagation co-ordinate z within the amplifier when there were n photons at the amplifier input ($z = 0$). In fact, $P_{n,m}(z)$ is a conditioned probability density function, hereafter called $P_m(z)$, and the differential equation it verifies is

$$v\frac{dP_m(z)}{dz} = \frac{Am}{1+sm}P_{m-1}(z) - \left[\frac{A(m+1)}{1+s(m+1)} + \frac{Bm}{1+sm} + Cm\right]P_m(z) + \left[\frac{B(m+1)}{1+s(m+1)} + C(m+1)\right]P_{m+1}(z) \qquad (1)$$

where A and B are the photon stimulated emission and absorption coefficients, respectively, C is a coefficient representing the nonsaturable absorption (linear losses in the amplifier medium), s is the saturation parameter, and v is the light velocity in the medium.

The method developed in this work deals with the master equation (eqn. 1) directly, and hence the complete profile of the probability density function (PDF) of the photon number at the output of a TWOA can be calculated. In this sense, we focus here on the discrepancies observed when using the usual Gaussian appoximation of the probability density function at the amplifier output rather than the 'real' statistics. A more exact calculation of the error probability in lightwave systems incorporating TWOAs could be a further application of this work.

Resolution method: A finite-difference equation can be obtained from eqn. 1 by approximating the derivative with respect to z by a difference quotient. After reordering the terms, we obtain

$$a_m P_{m-1,j+1} + b_m P_{m,j+1} + c_m P_{m+1,j+1} = -P_{m,j} \quad (2)$$

where $P_{m,j} \equiv P_m(j\Delta z)$, j being an integer index ($j = 0, 1, 2, \ldots, J$) denoting each discrete z co-ordinate and Δz the integration step, which is a fraction of the total amplifier length L ($\Delta z \equiv L/J$). a_m, b_m and c_m are defined as

$$a_m \equiv \frac{\Delta z}{v} \frac{Am}{1 + sm} \quad (3a)$$

$$b_m \equiv -1 - \frac{\Delta z}{v}\left[\frac{A(m+1)}{1 + s(m+1)} + \frac{Bm}{1 + sm} + Cm\right] \quad (3b)$$

$$c_m \equiv \frac{\Delta z}{v}\left[\frac{B(m+1)}{1 + s(m+1)} + C(m+1)\right] \quad (3c)$$

The PDF of the photon number which propagates through a TWOA is numerically calculated by varying the photon number from the value $m = 0$ to $m = M$. A sensible choice for M will depend on further calculations such as the accuracy degree required for the computation of the bit error probability at the amplifier output. In any case, a correct value for M can be found after a few iterations. The PDF for a fixed step index j is achieved by numerically solving a linear system of $M + 1$ equations obtained from eqn. 2 where $m = 0, 1, 2, \ldots, M$. Writing the system in matrix notation yields to a tridiagonal matrix, that is

$$\begin{pmatrix} b_0 & c_0 & 0 & 0 & 0 & \cdots & 0 \\ a_1 & b_1 & c_1 & 0 & 0 & \cdots & 0 \\ 0 & a_2 & b_2 & c_2 & 0 & \cdots & 0 \\ & & \vdots & \vdots & \vdots & & \\ 0 & 0 & 0 & \cdots & 0 & a_M & b_M \end{pmatrix} \begin{pmatrix} P_{0,j+1} \\ P_{1,j+1} \\ P_{2,j+1} \\ \vdots \\ P_{M,j+1} \end{pmatrix} = -\begin{pmatrix} P_{0,j} \\ P_{1,j} \\ P_{2,j} \\ \vdots \\ P_{M,j} \end{pmatrix} \quad (4)$$

The solution to the system of equations, i.e. the vector with step index $j + 1$, can be found by forward and backward substitution after the LU decomposition has been carried out [5].

Finally, the computation of the PDF at the output of a TWOA only needs the iteration of this resolution method starting from $j = 0$ (i.e. $z = 0$, amplifier input) to $j = J$ (i.e. $z = L$, amplifier output). For $j = 0$, the initial condition $P_{m,0}$, is in fact the discrete PDF of the input photon number n, i.e. $P(m = n)$.

Results and discussion: The complete profile of the PDF of the photon number at the amplifier output can be computed for any given arbitrary input photon number distribution. Here we focus on the comparison of the obtained PDF with its respective Gaussian approximation which has been calculated starting from its mean and variance. The semiconductor optical amplifier we have characterised has typical parameters $L = 500\,\mu m$, $s = 10^{-4}$, $A = 1{\cdot}6 \times 10^{12}\,s^{-1}$, $B = 4{\cdot}8 \times 10^{11}\,s^{-1}$, $C = 4 \times 10^{11}\,s^{-1}$ and $v = 8 \times 10^7$ m/s. We will consider two different situations regarding the absence and the presence of an input coherent light. The computation has been carried out using $M = 20\,000$ and $J = 1000$ for all the curves.

Fig. 1 shows the case of a zero input photon mean number (i.e. $\langle n \rangle = 0$) which corresponds to an input delta function distribution for which $P_{0 \cdot 0} = 1$, whereas $P_{m,0} = 0$ for $m \neq 0$. Logically, the PDF at the output of the amplifier (solid line) follows a Bose–Einstein distribution according to the random behaviour of the amplified spontaneous emission [6]. The dashed line corresponds to the Gaussian approximation of the PDF starting from its mean and variance. As expected, there is a marked discrepancy.

Fig. 2 shows in semilogarithmic scales the PDF for the case of input coherent lights, that is, input Poisson distributions. The solid lines stand for PDFs calculated with the new method (curves (i)–(iii)), and the dashed lines represent their corresponding Gaussian approximation (curves (i)′–(iii)′). The plots in Fig. 2 illustrate how the light statistics at the amplifier output approaches a Gaussian distribution as the input photon mean number increases from $\langle n \rangle = 10$ (curves (i)–(i)′) to $\langle n \rangle = 200$ (curves (iii) and (iii)′). This means that the discrepancy observed between the output PDF and the corresponding Gaussian approximation diminishes as the amplifier evolves from a quasilinear regime (weakly saturated, i.e. $sm \ll 1$) to a nonlinear regime (highly saturated, i.e. the product sm approaches, and even surpasses, unity).

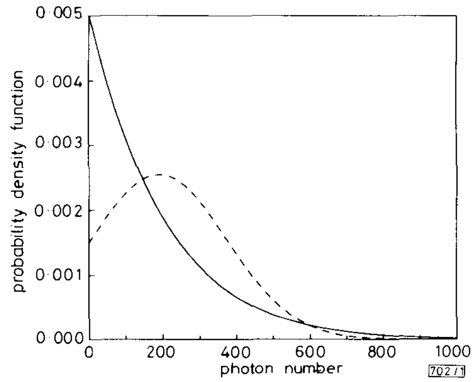

Fig. 1 *Probability density function of photon number for zero input photon mean number*

——— calculated with new method
– – – – Gaussian approximation

Note that the FORTRAN program we have implemented for the calculation of the PDF requires a total CPU time of $\sim(6{\cdot}3 \, . \, M \, . \, J) \times 10^{-6}$ s per PDF when running in a CONVEX computer machine, which represents approximately 2 min for each solid curve in Fig. 1 and Fig. 2.

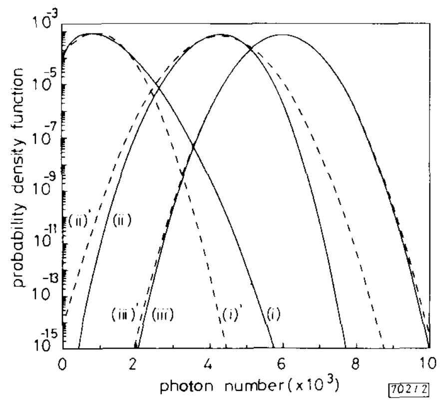

Fig. 2 *Probability density function of photon number for different input Poisson statistics*

——— new method
– – – – corresponding Gaussian approximations
(i), (i)′ $\langle n \rangle = 10$
(ii), (ii)′ $\langle n \rangle = 100$
(iii), (iii)′ $\langle n \rangle = 200$

In summary, we have developed a powerful method, based on linear algebra techniques, that operates with tridiagonal matrices which are simple to handle and, hence, with numerical calculations easy to implement in a computer. Moreover, the complete profile of the probability density function can be calculated whatever the saturation of the amplifier is. The main conclusion is that, with the proposed method, we have shown quantitatively that the customary Gaussian approximation is not always valid, at least when the input photon mean number is small.

9th July 1993

J. Guitart and S. Ruiz-Moreno (*Signal Theory and Communications Department, Polytechnic University of Catalonia, UPC Campus Nord—Edificio D5, c/ Sor Eulalia de Anzizu s/n 08034 Barcelona, Spain*)

References

1 WANG, Y. K., and LAMB, W. E. JR.: 'Quantum theory of an optical maser. VI. Transient behaviour', *Phys. Rev. A*, 1973, **8**, pp. 866–873
2 OLIVER, G., and BENDJABALLAH, C.: 'Statistical properties of coherent radiation in a nonlinear optical amplifier', *Phys. Rev. A*, 1980, **22**, pp. 630–634
3 YAMAMOTO, Y.: 'AM and FM quantum noise in semiconductor lasers—Part I: Theoretical analysis', *IEEE J. Quantum Electron.*, 1983, **QE-19**, pp. 34–46
4 RUIZ-MORENO, S., JUNYENT, G., USANDIZAGA, J. R., and CALZADA, A.: 'Resolution of moment equations in a nonlinear optical amplifier', *Electron. Lett.*, 1987, **23**, pp. 15–17
5 DAHLQUIST, G., and BJÖRK, A.: 'Numerical methods' (Prentice-Hall, Series in Automatic Computation, 1974)
6 DIAMENT, P., and TEICH, M. C.: 'Evolution of the statistical properties of photons passed through a traveling-wave laser amplifier', *IEEE J. Quantum Electron.*, 1992, **QE-28**, pp. 1325–1334

ERRATA

OSHRI, E., SHELLY, N., and MITCHELL, H. B.: 'Interpolative three-level block truncation coding algorithm', *Electron. Lett.*, 1993, **29**, (14), pp. 1267–1268

Editor's correction

In eqns. 5, the multiplication signs should be replaced by the letter x

Authors' corrections

In the second of eqns. 5, the minus signs should be replaced by plus signs

In the last column of Table 2, the figures 1·22 and 1·07 should be interchanged

In the title of Table 3, the words 'on Lena' should be inserted after 'obtained'

In the notes to Table 3, '*SNR*' should be defined as the signal-to-noise ratio, dB. In the definitions of BTC-1 and BTC-2, 'truncation blocks' should read 'truncation block values'

ESTIMATION OF LENGTH FOR *ELECTRONICS LETTERS*

Title + Abstract	4 col cm
Authors	2 col cm per address
Text	1 col cm per 165 characters Estimate number of characters (including spaces) per line and number of lines per page. Add 0·5 or 1 col cm for each equation unless it is well displayed; similarly for each line in a matrix
Tables	1 col cm for title, 0·5 col cm for each line (including blanks). Double up for wide (double column) tables
Figure captions	1 col cm for main caption. 0·33 col cm per line for subcaptions, including keys which would be moved from the graphics
Figures	These are usually reduced to single column width as per this table:

Width (inches)	Reduction (%)
Less than 3·5	95
3·5–4·4	75
4·4–5·3	62
5·3–6·1	54
6·1–7·0	47
7·0–8·9	37
8·9–10·6	31
10·6–12·2	27

If the figure needs to be reproduced over two columns the result of the above calculation must be multiplied by *four*

References	1 col cm each